Micromagnetic study of inertial spin waves in ferromagnetic nanodots

Massimiliano d'Aquino, Salvatore Perna, Matteo Pancaldi, Riccardo Hertel, Stefano Bonetti, Claudio Serpico

Micromagnetic study of inertial spin waves in ferromagnetic nanodots

Massimiliano d'Aquino,[1] Salvatore Perna,[1] Matteo Pancaldi,[2,3]
Riccardo Hertel,[4] Stefano Bonetti,[2] and Claudio Serpico[1]

[1] *Department of Electrical Engineering and ICT, University of Naples Federico II, Naples, Italy**
[2] *Department of Molecular Sciences and Nanosystems, Ca' Foscari University of Venice, 30172 Venice, Italy*
[3] *Elettra-Sincrotrone Trieste S.C.p.A., 34149 Basovizza, Trieste, Italy*
[4] *Université de Strasbourg, CNRS, Institut de Physique et Chimie des Matériaux de Strasbourg, F-67000 Strasbourg, France*

(Dated: April 4, 2023)

Here we report the possibility to excite ultra-short spin waves in ferromagnetic thin-films by using time-harmonic electromagnetic fields with terahertz frequency. Such ultra-fast excitation requires to include inertial effects in the description of magnetization dynamics. In this respect, we consider the inertial Landau-Lifshitz-Gilbert (iLLG) equation and develop analytical theory for exchange-dominated inertial spin waves. The theory predicts a finite limit for inertial spin wave propagation velocity, as well as spin wave spatial decay and lifetime as function of material parameters. Then, guided by the theory, we perform numerical micromagnetic simulations that demonstrate the excitation of ultra-short inertial spin waves (20 nm long) propagating at finite speed in a confined magnetic nanodot. The results are in agreement with the theory and provide the order of magnitude of quantities observable in realistic ultra-fast dynamics experiments.

I. INTRODUCTION

The study of ultra-fast magnetization processes is a central issue in spin dynamics for its potential application to future generations of nanomagnetic and spintronic devices[1]. In the last decades, after the pioneering experiment[2] revealing subpicosecond spin dynamics, the investigation of ultra-fast magnetization processes has increasingly attracted the attention of many research groups stimulating the production of considerable research[3–10].

Recently, the direct detection of spin nutation in ferromagnets achieved experimentally[11, 12] in the terahertz range has confirmed the presence of inertial effects in magnetization dynamics which were theoretically predicted[13–15] several years ago. In the past decades, nutation-type magnetization motions in nanomagnets were also studied theoretically within the classical dynamics occurring at gigahertz frequencies[16]. Besides its fundamental implications for the physics of magnetism, terahertz spin nutation opens the way to study possible exploitation of novel ultra-fast regimes for technological applications such as, for instance, ballistic magnetization switching[17–20] driven by strong picosecond field pulses into the inertial regime[21, 22].

From the theoretical point of view, inertial magnetization dynamics can be modeled by augmenting the classical Landau-Lifshitz-Gilbert (LLG) precessional dynamics with a torque term taking into account angular momentum relaxation[13], which is able to explain the observed nutation dynamics[11] in homogeneously-magnetized samples. When spatial changes of magnetization are allowed in magnetic systems of nano- and micro-scale, the issue of the emergence of inertial spin waves oscillating at terahertz frequency arises. In this respect, very recently a number of theoretical studies have been performed to characterize nutation spin waves[23–30]. These interesting studies are mostly concerned with the analysis of spin waves propagation in infinite media. However, the realization of nanoscale magnetic devices such as, for instance, memories or computing units, does intrinsically involve confined nanostructures.

In this paper, we investigate, by using full micromagnetic simulations of inertial LLG (iLLG) dyanmics, the excitation of ultra-short inertial spin waves in a confined ferromagnetic nanodot under the action of terahertz fields. We first derive suitable dispersion relation under the assumption of exhange-dominated spin waves, then perform full micromagnetic ac steady-state analysis of magnetization response to assess the onset of nutation resonance at certain terahertz frequency. By choosing an excitation frequency larger than such nutation resonance, we demonstrate the possibility to excite short-wavelength (i.e. 20 nanometers long) nutation spin waves. Finally, we simulate realistic time-domain magnetization processes driven by subpicosecond excitation which reveal the finite speed propagation of these ultra-short inertial spin waves in possible experiments.

II. MODEL OF INERTIAL SPIN WAVE DYNAMICS

Magnetization dynamics is described by the iLLG equation, which can be written in normalized form as follows[11, 13, 21, 31]:

$$\frac{\partial \boldsymbol{m}}{\partial t} = -\boldsymbol{m} \times \left(\boldsymbol{h}_{\text{eff}} - \alpha \frac{\partial \boldsymbol{m}}{\partial t} - \xi \frac{\partial^2 \boldsymbol{m}}{\partial t^2} \right) , \qquad (1)$$

* mdaquino@unina.it

where magnetization is expressed by the unit-vector $\boldsymbol{m}(\boldsymbol{r},t)$ normalized by the saturation magnetization M_s, time is measured in units of $(\gamma M_s)^{-1}$ (γ is the absolute value of the gyromagnetic ratio), $\boldsymbol{h}_{\text{eff}}$ is the micromagnetic effective field (also normalized by M_s) which includes contributions arising from different interaction (exchange, anisotropy, magnetostatic, Zeeman) terms in the free energy, α is the Gilbert damping parameter, and ξ measures the strength of inertial effects. We remark that this dimensionless quantity can be written as $\xi = (\gamma M_s \tau)^2$ and, in this respect, it determines the physical time-scale τ of inertial effects, which according to previous studies[11, 13, 21] has the order of magnitude of fractions of picosecond (meaning $\xi \sim 10^{-2}$). Thus, the inertia in magnetization dynamics is controlled by a small quantity comparable with usual Gilbert damping $\alpha \sim 10^{-2}$.

Although the inertial effects represent a small term in eq. (1), the iLLG dynamics is significantly different from classical precessional dynamics in that emergence of ultra-fast nutation appears at terahertz frequencies, which opens the possibility to access novel dynamical magnetization regimes. In the sequel, we will focus the attention on the possibility to drive the excitation of ultra-short spin waves in ferromagnetic thin-films.

To this end, we will first consider the idealized situation of indefinite magnetic thin-film and derive the spin wave dispersion relation for small-amplitude spin waves in the exchange-dominated case. For the sake of simplicity, we consider small magnetization oscillations around a spatially-uniform in-plane equilibrium $\boldsymbol{m}_0$ such as that obtainable by saturating the thin-film with a static external field $\boldsymbol{h}_a$. By posing $\boldsymbol{m}(\boldsymbol{r},t) = \boldsymbol{m}_0 + \delta\boldsymbol{m}(\boldsymbol{r},t)$ and linearizing eq. (1) around $\boldsymbol{m}_0$, one has:

$$\frac{\partial \delta\boldsymbol{m}}{\partial t} = -\boldsymbol{m}_0 \times \left(\delta\boldsymbol{h}_{\text{eff}} - h_0 \delta\boldsymbol{m} - \alpha \frac{\partial \delta\boldsymbol{m}}{\partial t} - \xi \frac{\partial^2 \delta\boldsymbol{m}}{\partial t^2} \right), \tag{2}$$

where $\delta\boldsymbol{m} \cdot \boldsymbol{m}_0 = 0$ (at first-order), $\delta\boldsymbol{h}_{\text{eff}}$ only includes linear terms in the magnetization deviation $\delta\boldsymbol{m}$ (typically exchange, magnetostatics, uniaxial anisotropy) and $h_0 = h_a + \kappa_{\text{an}} > 0$ (κ_{an} is the normalized uniaxial anisotropy constant, if applicable). The assumption of indefinite thin-film allows to consider description of magnetization perturbation $\delta\boldsymbol{m}$ in terms of plane waves via Fourier approach. Since we are interested in the study of short wavelength spin waves oscillating at terahertz frequency, we neglect magnetostatics in eq. (2) assuming $\delta\boldsymbol{h}_{\text{eff}} = l_{\text{ex}}^2 \nabla^2 \delta\boldsymbol{m}$ (with $l_{\text{ex}} = \sqrt{2A/(\mu_0 M_s^2)}$ and A being the exchange constant of the material). We consider an in-plane magnetization equilibrium $\boldsymbol{m}_0 = \boldsymbol{e}_x$ ($\boldsymbol{e}_x$ is the cartesian unit-vector along the x axis) and consider for simplicity magnetization deviations $\delta\boldsymbol{m}(x,t)$ with spatial changes occurring only along the x axis. In this situation, one can perform two-dimensional Fourier transform of eq.(2) leading to:

$$i\omega \delta\hat{\boldsymbol{m}} = -\boldsymbol{e}_x \times (-k^2 l_{\text{ex}}^2 - h_0 - i\alpha\omega + \xi\omega^2)\delta\hat{\boldsymbol{m}} \tag{3}$$

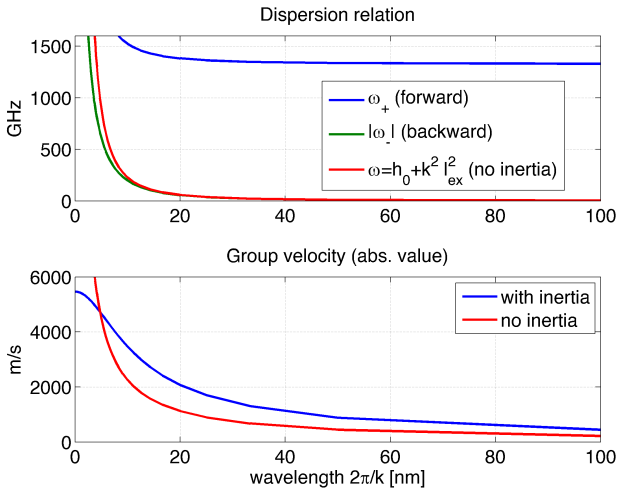

FIG. 1. Dispersion relation for spin waves. Top panel reports $|\omega_\pm|$ according to eq.(6) along with the classical exchange-dominated spin wave dispersion relations. The bottom panel reports the associated group velocities. The value of parameters are $\gamma = 2.211 \times 10^5$ m A^{-1} s^{-1}, $\mu_0 M_s = 1.6$ T, $A = 13$ pJ/m ($l_{\text{ex}} = 3.57$ nm), $\tau = 0.653$ ps ($\xi = 0.0338$) and $h_0 = 0.0625$. Notice the approach to the limiting value $v_g(k \to \infty) = l_{\text{ex}}/\tau \approx 5470$ m/s in the short wavelength limit.

where $\delta\hat{\boldsymbol{m}} = \iint_{\mathbb{R}^2} \delta\boldsymbol{m}(x,t) e^{i(kx-\omega t)}\, dx\, dt$. By expressing $\delta\hat{\boldsymbol{m}} = \delta\hat{m}_y \boldsymbol{e}_y + \delta\hat{m}_z \boldsymbol{e}_z$ and introducing the notation $\hat{\psi} = \delta\hat{m}_y + i\delta\hat{m}_z$, the latter equation becomes:

$$(-\omega - k^2 l_{\text{ex}}^2 - h_0 - i\alpha\omega + \xi\omega^2)\hat{\psi} = 0\,. \tag{4}$$

Equation (4), in the lossless limit $\alpha = 0$, admits non-trivial solutions when the quantity in parenthesis vanishes:

$$\omega^2 - \frac{\omega}{\xi} - \frac{k^2 l_{\text{ex}}^2}{\xi} - \frac{h_0}{\xi} = 0\,. \tag{5}$$

The solution of eq.(5) yields the dispersion relation (the angular frequency ω is measured in units of γM_s):

$$\omega_\pm = \frac{1}{2\xi}\left(1 \pm \sqrt{1 + 4(h_0 + k^2 l_{\text{ex}}^2)\xi}\right), \tag{6}$$

which apparently is composed of two different branches (we remark that choosing $\hat{\psi} = \delta\hat{m}_y - i\delta\hat{m}_z$ yields the opposite of eq.(6)). The lower frequency branch $|\omega_-|$ represents the deviation from the classical exchange-dominated dispersion relation $\omega = h_0 + k^2 l_{\text{ex}}^2$ starting at the (Kittel) ferromagnetic resonance (FMR) frequency

$$\omega_K = |\omega_-| \overset{k\to 0}{=} \left|\frac{1 - \sqrt{1 + 4h_0\xi}}{2\xi}\right| \overset{\xi \ll 1}{\approx} |-h_0 + h_0^2 \xi|\,, \tag{7}$$

where the weak influence of inertia is also recognizable. Conversely, the higher frequency branch ω_+ describes

intrinsic features of inertial dynamics occurring at frequencies larger than the following nutation resonance frequency:

$$\omega_N = \omega_+ \overset{k\to 0}{=} \frac{1}{2\xi}\left(1+\sqrt{1+4h_0\xi}\right) \overset{4h_0\xi\ll 1}{\approx} \frac{1}{\xi}+h_0\,. \quad (8)$$

It is also worth noting that both branches of the dispersion relation (6) give rise to the same group velocity (except for the sign):

$$v_g(k) = \gamma M_s \frac{\partial \omega}{\partial k} = \pm \frac{\gamma M_s\, 2k l_{\rm ex}^2}{\sqrt{1+4(h_0+k^2 l_{\rm ex}^2)\xi}}\,, \quad (9)$$

which remarkably approaches a finite value in the limit of short wavelength $k\to\infty$:

$$v_g(k\to\infty) = v_{g,\infty} = \frac{\gamma M_s\, l_{\rm ex}}{\sqrt{\xi}} = \frac{l_{\rm ex}}{\tau}\,. \quad (10)$$

It is interesting to estimate the order of magnitude of the speed limit expressed by eq.(10); by choosing $\gamma = 2.211\times 10^5$ m A^{-1} s^{-1}, $\tau = 0.653$ ps, $\mu_0 M_s = 1.6$ T, $A = 13$ pJ/m, one has $v_{g,\infty}\approx 5470$ m/s.

The dispersion relation and the group velocity expressed by eqs.(6)-(9) are depicted in fig.1 using the aforementioned material parameters of fcc Cobalt reported in Ref.[12]. We observe that neglecting inertial effects produces unlimited group velocity in the short wavelength limit (red line in bottom panel of fig.1 will diverge for vanishing wavelength, i.e $k\to\infty$). Conversely, the inertial spin waves related to both branches will approach the same limiting speed in the limit of large wavenumber (i.e. for $k\to\infty$, blue line will approach the value $v_{g,\infty}$ of eq.(10)).

Equation (4) provides additional insight when nonzero damping $\alpha\neq 0$ is considered. In fact, its nontrivial solutions obey the following equation:

$$\xi\omega^2 - \omega(1+i\alpha) - k^2 l_{\rm ex}^2 - h_0 = 0\,. \quad (11)$$

For a given frequency ω, one can solve for the complex $k = k_\pm + i\delta k_\pm$ and obtain, in the limit $\alpha\ll 1$, the wavenumber $k_\pm = \Re\{k\}$ and the spatial decay constant $\sigma_\pm = -\delta k_\pm = -\Im\{k\}$ of the plane wave e^{-ikx} associated with the frequency ω, respectively:

$$k_\pm = \pm\frac{\sqrt{\xi\omega^2-\omega-h_0}}{l_{\rm ex}} + \mathcal{O}(\alpha^2)\,, \quad (12)$$

$$\delta k_\pm = \mp\frac{\alpha\omega}{2l_{\rm ex}\sqrt{\xi\omega^2-\omega-h_0}} + \mathcal{O}(\alpha^2)\,. \quad (13)$$

It is apparent that, at first order, $k_\pm$ does not depend on α whereas $\delta k_\pm$ is proportional to α as expected. Furthermore, by solving eq.(11) for small $\alpha\neq 0$, one can derive the time decay constant $\delta\omega_\pm$:

$$\delta\omega_\pm = \frac{\alpha}{2\xi}\left(1\pm\frac{1}{\sqrt{4\xi k^2 l_{\rm ex}^2+4h_0\xi+1}}\right)\,, \quad (14)$$

(a)

Quantity	Equation
iSW dispersion relation $\omega_\pm(k)$ (units of γM_s)	(6)
FMR frequency ω_K vs inertia ξ and static field h_0	(7)
FMR linewidth $\Delta\omega_K$ vs α,ξ,h_0	(16)
nutation resonance frequency ω_N vs ξ,h_0	(8)
nutation resonance linewidth $\Delta\omega_N$ vs α,ξ,h_0	(15)
group velocity $v_g(k)$ vs $\gamma, M_s, \xi, h_0, l_{\rm ex}$	(9)
limit group velocity $v_{g,\infty} = v_g(k\to\infty)$	(10)
iSW wavenumber $k_\pm$ vs $\xi,\omega,h_0,l_{\rm ex}$	(12)
iSW exp. spatial decay $\sigma_\pm = -\delta k_\pm$ vs $\alpha,\xi,\omega,h_0,l_{\rm ex}$	(13)
iSW exp. time decay $\delta\omega_\pm$ vs $\alpha,\xi,\omega,h_0,l_{\rm ex}$	(14)

(b)

Parameter	Better choice
damping α	low
exchange length $l_{\rm ex} = \sqrt{2A/(\mu_0 M_s^2)}$	high
inertia $\xi = (\gamma M_s \tau)^2$	high
static field/anisotropy h_0 (weak dependence)	low

TABLE I. (a) Summary of theoretical predictions and reference to equations in main text for quantities related with inertial spin waves (iSW) as function of material parameters. (b) Influence of parameters on excitation of short-wavelength inertial spin-waves with low spatial decay and long lifetime arising from inspection of eqs.(12)-(15)

.

which provides information on the temporal duration of the spin-wave as function of parameters. In particular, we remark that $2\delta\omega_+$ yields a simple estimate for the full-width half maximum (FWHM) linewidth $\Delta\omega_N$ of the power spectrum around the nutation resonance ω_N defined by eq.(8), namely:

$$\Delta\omega_N = 2\delta\omega_+ \overset{k\to 0}{=} \frac{\alpha}{\xi}\left(1+\frac{1}{\sqrt{4h_0\xi+1}}\right) \overset{4h_0\xi\ll 1}{\approx} \frac{2\alpha}{\xi} - 2\alpha h_0\,, \quad (15)$$

where a weak dependence on h_0 (static external field and/or uniaxial anisotropy) appears. Analogously, one can derive the spectral linewidth $\Delta\omega_K$ of (Kittel) ferromagnetic resonance (FMR) in the presence of inertia:

$$\Delta\omega_K = 2\delta\omega_- \overset{k\to 0}{=} \frac{\alpha}{\xi}\left(1-\frac{1}{\sqrt{4h_0\xi+1}}\right) \overset{4h_0\xi\ll 1}{\approx} 2\alpha h_0 - 6\alpha h_0^2\xi\,. \quad (16)$$

The developed theory, whose main equations are summarized in table I(a), can be instrumental for determining the conditions, in terms of material parameters and external excitation, suitable to excite spin-waves in the inertial regime. First, it is expected that, in order to excite spin-waves with low spatial decay and long lifetime, one needs material with very small damping. This is confirmed by eqs.(12)-(15). In addition, eq.(13) reveals less obvious inverse dependence of the spin-wave decay $\sigma_\pm = -\delta k_\pm$ on the exchange length $l_{\rm ex} = \sqrt{2A/(\mu_0 M_s^2)}$, which may favor materials with smaller saturation magnetization M_s. A summary of the influence of parameters suitable to produce inertial spin waves is provided in table I(b). The completely new picture arising from inertial dynamics involves frequencies spanning the tera-

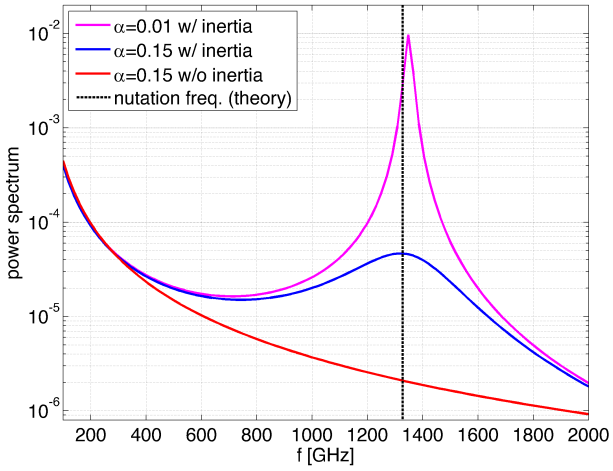

FIG. 2. Power spectrum of magnetization computed by micromagnetic simulations according to eq.(17). Magenta and blue (red) lines refer to the presence (absence) of inertial effects in magnetization dynamics for different values of damping. The dashed black line refers to theoretical estimate (8) for nutation resonance frequency $f_N \approx 1328$ GHz. FWHM nutation linewidths predicted by eq.(15) are approximately 26.5 GHz and 397 GHz for $\alpha = 0.01$ and $\alpha = 0.15$, respectively, in agreement with the results of micromagnetic simulations (27.1 GHz and 401 GHz).

hertz range above the nutation resonance frequency ω_N (see eq.(8)) that, for the chosen parameters of fig.1, yields approximately $f_N \approx 1328$ GHz. For this reason, in the sequel we investigate spin wave dynamics occurring at frequency larger than the nutation resonance f_N.

III. MICROMAGNETIC SIMULATIONS

In order to assess the excitation of ultra-short wavelength inertial spin waves, we perform two independent studies, one in the frequency domain and the other in the time domain, involving a square $200 \times 200 \times 5$ nm^3 thin-film nanodot, with the same material parameters as those of fig.1, saturated along the x axis by a static field $\mu_0 H_{ax} = 100$ mT. In the former situation, we investigate ac steady-state magnetization dynamics for the aforementioned nanodot driven by a spatially-uniform linearly-polarized ac field transverse to the equilibrium magnetization with frequency $f = 1386$ GHz and amplitude $\mu_0 H_{ay} = 100$ mT. The magnetization is initially in the remanent equilibrium configuration under the static external magnetic field, which is mainly oriented along the x axis with deviations located close to the thin-film edges parallel to the y axis.

A. Frequency-domain study

The ac forced magnetization dynamics can be conveniently studied by solving the linearized iLLG in the frequency domain and determining the frequency response and the power spectrum. Here we use a finite-difference frequency-domain large-scale micromagnetic solver[32] based on suitable operator formalism[33], appropriately extended in order to include inertial effects and implemented in the numerical code MaGICo[34]. The output of the code is the steady-state ac magnetization response $\delta\hat{\boldsymbol{m}}(\boldsymbol{r})$ (such that $\delta\boldsymbol{m}(\boldsymbol{r},t) = \mathcal{R}\{\delta\hat{\boldsymbol{m}}(\boldsymbol{r})\exp(i\omega t)\}$) computed for desired values of the external ac field frequency ω (see ref.[32] for further details). For each given ω, the ac power spectrum of magnetization is then computed as[32]:

$$p(\omega) = \frac{1}{V}\int_\Omega \frac{|\delta\hat{\boldsymbol{m}}(\boldsymbol{r})|^2}{2}\,dV \approx \frac{1}{N}\sum_{j=1}^{N}\frac{|\delta\hat{\boldsymbol{m}}_j|^2}{2}\,, \qquad (17)$$

where V is the volume of the region Ω occupied by the magnetic body, discretized with N computational prism cells of identical volume (in the present case we use $2.5 \times 2.5 \times 5$ nm^3 cells).

The ac power spectrum of magnetization, computed according to eq.(17) in the terahertz frequency range, is reported in fig.2 as function of the damping α. It is apparent that there is a spectral peak owing to nutation resonance close to the theoretical value $f_N \approx 1328$ GHz (dashed vertical black line in fig.2), while no such peak appears in the classical precessional ac-driven LLG dynamics. FWHM nutation linewidths predicted by eq.(15) (26.5 GHz and 397 GHz for $\alpha = 0.01$ and $\alpha = 0.15$, respectively) are also in agreement with those computed from micromagnetic simulations (27.1 GHz and 401 GHz, respectively). We have used material parameters for fcc Cobalt such as those reported in a recent experimental work[12], where a quite large damping $\alpha = 0.15$ was estimated from the measurements of nutation frequency response.

With that in mind, we follow the predictions of the developed theory concerning short-wavelength spin waves and, therefore, we explore the magnetization response at frequency $f = 1386$ GHz. In this respect, eq.(12) for the above frequency predicts a wavelength of 20 nm for the excited spin-waves. However, eq.(13) particularized with $\alpha = 0.15$ yields a spatial decay constant σ_+ such that the excited spin-waves would be exponentially attenuated by more than two orders of magnitude within a distance $\sim 5/\sigma_+$ which is less than 10 nm, meaning that nutation waves would not be observable in this condition. Thus, according to eq.(13), in order to have spin waves that are 20 nm long and can extend for hundred nanometers, one needs materials with damping in the order of $\alpha \sim 10^{-2}$. Moreover, as predicted by eq.(13) and reported in table I, the detrimental effect of large damping could be mitigated, in principle, by using materials with larger exchange length (i.e. smaller saturation magnetization).

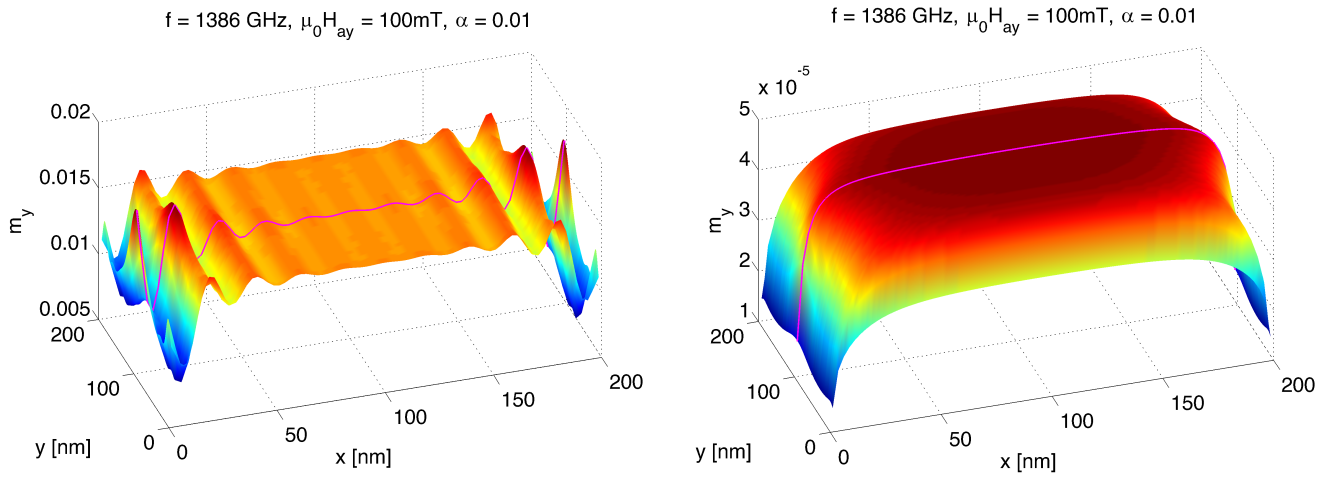

FIG. 3. Snapshot at $t = 0$ of steady-state in-plane ac magnetization response m_y at driving frequency $f = 1386$ GHz. The color code represents the value of m_y at each spatial location ranging from minimum (blue) to maximum (red). Left panel refers to inertial LLG dynamics while right panel refers to classical LLG dynamics. Magenta solid lines refer to $m_y(x)$ sampled in the middle of the nanodot at $y = 100$nm.

In this respect, Cobalt seems not to be the best choice, since it has notably quite small value of $l_{\rm ex} \approx 3.57$ nm due to its large saturation magnetization such that $\mu_0 M_s = 1.6$ T.

The result of micromagnetic simulations with $\alpha = 0.01$ is reported in fig.3. One can clearly see (left panel of fig.3) that inertial spin wave dynamics driven at frequency $f > f_N$ involves ultra-short nutation spin waves with wavelength around 20 nm (one can count roughly ten oscillation periods along the x direction), which is in excellent agreement with the dispersion relation eq.(6) (see fig.1). As expected, the excitation frequency only matches the upper branch of eq.(6). On the other hand, when inertia is not considered (right panel of fig.3), the oscillation amplitude is two orders of magnitude smaller than in the inertial case, and short spin waves are not excited anymore.

The time-evolution of the ac steady-state magnetization $\delta\boldsymbol{m}(\boldsymbol{r},t) = \mathcal{R}\{\delta\hat{\boldsymbol{m}}(\boldsymbol{r})\exp(i\omega t)\}$ basically consists of a superposition of two oscillations, the former having almost spatially-uniform profile and the other with wavelength around 20 nm. One can interpret the former as describing spatially-uniform magnetization nutation and the second being the spatially-inhomogeneous magnetization nutation ascribed to the excitation of inertial spin waves. This can be also inferred observing the comparison between the spatial patterns of magnetization responses in the presence and absence of inertial effects, sampled at time $t = 0$ and reported in the two panels of fig.3. We immediately remark that the maximum amplitude of magnetization is significantly different in the two situations. This occurs since, in the inertial case, the external excitation at frequency 1386 GHz is close to the resonant peak (see also fig.2) that enhances the steady-state response of the system, compared with the situation of classical LLG precessional dynamics where there is no such resonance. Apart from the aforementioned situation, one can grasp the similarity between the long wavelength magnetization profiles. As far as the quantitative comparison of spin-wave amplitudes associated with spatially-uniform and nonuniform nutations is concerned, we have evaluated the relative difference between the power spectrum computed according to Eq.(17) from full micromagnetic simulations with that computed using Eq.(17) only with the spatially-averaged magnetization $\delta\hat{\boldsymbol{m}}_{\rm avg} = \frac{1}{N}\sum_{j=1}^{N}\delta\hat{\boldsymbol{m}}_j$, namely $p_{\rm avg}(\omega) = \delta\hat{\boldsymbol{m}}^2_{\rm avg}/2$. The relative difference $(p(\omega) - p_{\rm avg}(\omega))/p_{\rm avg}(\omega)$ is below one percent in the whole considered frequency range. De-

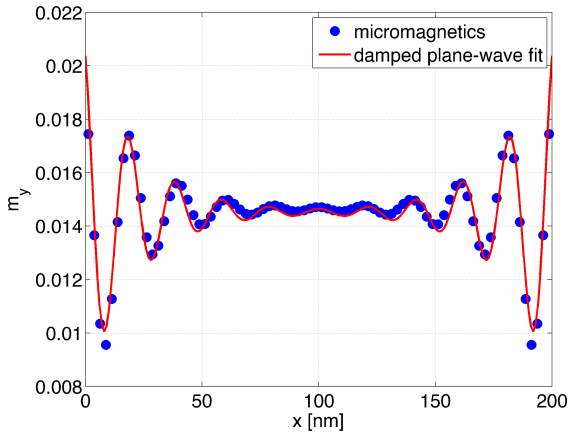

FIG. 4. Spatial profile along x axis of magnetization in-plane component m_y sampled at $t = 0$ along the middle line $y = L/2 = 100$ nm. Dots refer to micromagnetic simulation while solid line is a fit to the two damped plane wave ansatz eq.(18).

spite such a small relative weight in the power spectrum, the ultra-short spin-wave oscillation is clearly visible in figures 3 and 4.

In order to compare the theoretical prediction obtained in the ideal case of infinite thin-film with the results of simulations for confined structures, we have characterized the short inertial spin waves by fitting the spatial profile of the ac steady-state in-plane oscillation m_y (sampled along x in the middle line at $y = 100$nm) with the following two damped plane wave ansatz:

$$\psi(x) = a + b\frac{e^{-\sigma x}\cos(kx+\beta) + e^{-\sigma(x-L)}\cos(k(x-L)+\beta)}{2}, \tag{18}$$

where we have fixed $k = 2\pi/20$ rad/nm, $L = 200$ nm. The result is reported in table II and the comparison with simulations is reported in fig.4, showing nice agreement with the assumption of plane wave profile.

Parameter	Value	confidence intervals
a	0.01453	(0.0144, 0.01465)
b	0.01305	(0.01131, 0.01478)
β	0.4592	(0.3785, 0.54)
σ	0.04541	(0.03758, 0.05324)

TABLE II. Values of the fitting parameters for eq.(18). Notice that $k = 2\pi/20$ nm and $L = 200$ nm.

We observe that the spatial decay constant $\sigma \approx 0.045$ extracted from the fitting is in good agreement with the value $\sigma_+ \approx 0.0374$ predicted by eq.(13) despite the latter is based on the assumption of spatially-uniform equilibrium $\boldsymbol{m}_0$, whereas the actual equilibrium magnetization close to the boundaries of the nanodot has slightly different orientation compared to that in the center due to the magnetostatic field created by the magnetic charges arising from the confinement[35]. In addition, as mentioned before, we notice that the nonzero offset $a = 0.01453$ corresponds to a significant spatially-uniform component of $m_y(x)$, superimposed to the plane wave mode of maximum amplitude $b = 0.01305$, which is also associated with spatially-uniform magnetization nutation at the same frequency 1386 GHz.

B. Time-domain study

The results outlined in the previous section reveal the possibility to excite ultra-short spin waves by using ac terahertz excitation. However, full understanding of the profoundly different nature of inertial magnetization dynamics compared to the classical precessional dynamics can be achieved by complementing frequency-domain calculations with time-domain analysis of transient magnetization dynamics. This difference is apparent in the mathematical structure of eq.(1) compared with the same equation with $\xi = 0$. The torque proportional to the second-order derivative transforms the classical LLG equation into a wave-like equation with hyperbolic mathematical nature.

This means that inertia leads to wave propagation phenomena with finite speed. In this respect, we investigate the transient magnetization dynamics triggered by the action of a terahertz field step when the initial magnetic state is the static remanent equilibrium configuration.

To this end, we perform full micromagnetic simulations of eq.(1) using the finite-difference numerical code MaGICo[34, 36] which is able to perform fast and large-scale time-integration of iLLG dynamics. Thus, we integrate iLLG equation (1) with a time-step of 25 fs, a $2.5\times2.5\times5$ nm^3 computational cell, and record the space configuration of magnetization at each time-step. The applied field is a spatially-uniform sine wave step (turned on at $t = 0$) along the y axis transverse to the equilibrium configuration with the same amplitude $\mu_0 H_{ay} = 100$ mT and frequency $f = 1386$ GHz as in the frequency-domain study. Despite using the same excitation, the present situation offers the possibility to look at the propagation of inertial short-wavelength waves along the magnetic thin-film evidencing the finite time delay. We remark that the choice of a spatially-uniform excitation field is related with the possibility to realize this experiment with realistic laser sources that create a spot much larger than the dimension of the considered magnetic nanodot. The spatial uniformity of the applied field step obviously produces the transient excitation of a plethora of spin wave modes with very different wavelengths, which makes difficult the direct inspection of the inertial spin wave propagation. For this reason, also based on the agreement with the plane wave nature of inertial spin waves demonstrated by the frequency-domain simulations, we apply spatial high-pass Fast Fourier Transform (FFT) filter (the cutoff wavenumber is 0.2 rad/nm) to capture the evolution of short-wavelength spin waves. The so-obtained short wavelength magnetization patterns of the resulting out-of plane magnetization sampled along the middle line of the thin-film square at different time instants are reported in fig.5.

The initial equilibrium magnetization configuration lies in the sample plane with more pronounced deviations from the x orientation localized in the region close to the edges perpendicular to the static field (i.e. those at $x = 0$ and $x = 200$ nm). Then, one can clearly see from fig.5 that, when the sine wave step is applied, the magnetization response originates from the edges and gives rise to plane waves with wavelength around 20 nm propagating along the thin-film towards its center. The simulated experiment is repeated for two values of damping $\alpha = 0.005, 0.01$ to investigate spin wave spatial decay and for two ac field amplitudes $50, 100$ mT in order to check the linearity of the response. In this respect, on one hand one can clearly see in fig.5 that, for a given field amplitude, lower damping implies smaller spatial decay. On the other hand, it happens that doubling the ac field amplitude produces a magnetization response with doubled amplitude, which assesses the linear nature

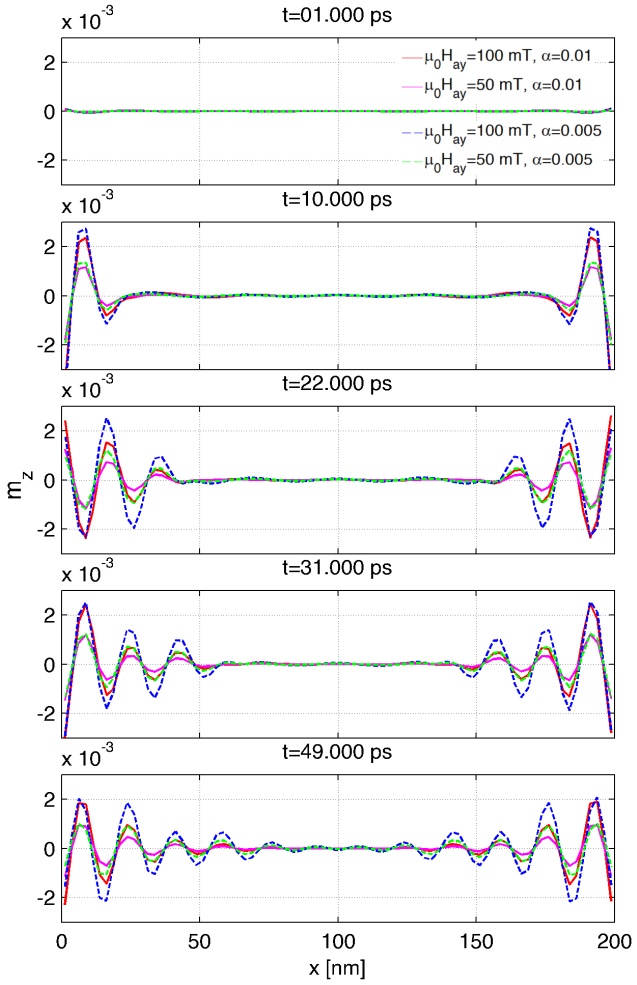

FIG. 5. Spatial profiles along x axis of short-wavelength magnetization out-of-plane component m_z as function of ac field amplitude and damping, obtained by FFT high-pass filtering, sampled at different time instants.

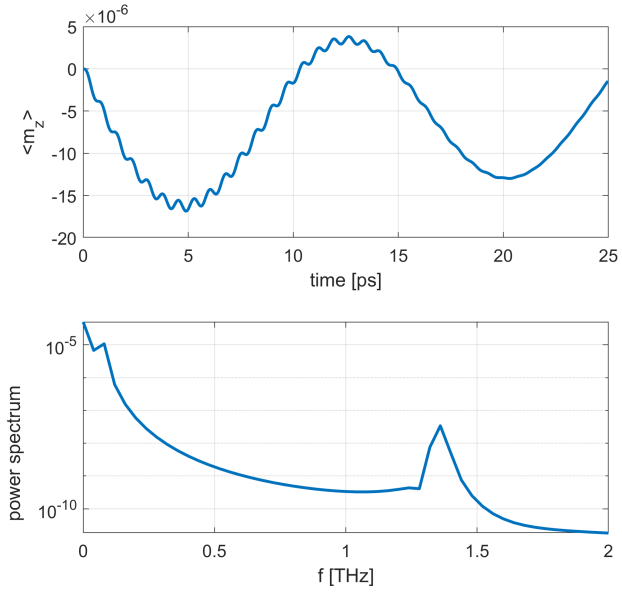

FIG. 6. Free magnetization response starting from periodically-modulated initial state with spatial period 20 nm. The upper panel reports the time-evolution of the spatially-averaged out-of-plane component $\langle m_z \rangle$, the lower panel reports the power spectrum (estimated by the periodogram, i.e. the squared amplitude of the FFT) of $\langle m_z \rangle$. Spectral peaks at about 60GHz and 1380 GHz are apparent.

of inertial spin-wave dynamics despite the application of terahertz ac fields with moderately large amplitude. Although the effect of damping produces the decay of the oscillation, it is also apparent that the two wavefronts of the forward and backward wavepackets approach the center of the square in around 49 picoseconds, which allows us to roughly estimate the group velocity of the inertial spin waves around 2040 m/s, which is in striking agreement with the theoretical prediction $v_g \approx 2080$ m/s given by eq.(9) for $k = 2\pi/20$ rad/nm. This value of speed amounts to slightly less than half the ultimate speed limit $v_{g,\infty} \approx 5470$ m/s predicted by eq.(10).

Finally, we perform an additional investigation of transient magnetization dynamics starting from an initial magnetization deviating from the saturated state by a periodically modulated wave, which can be instrumental to check the natural oscillation frequency associated with plane wave perturbations of given wavenumber. The outcome of the simulation starting from the initial state $\boldsymbol{m} = (1, \epsilon \sin(kx), 0)/\sqrt{1+\epsilon^2 \sin^2(kx)}$, with $k = 2\pi/20$ rad/nm and $\epsilon = 10^{-2}$) is reported in fig.6. One can clearly see in the upper panel that magnetization exhibits the composition of two oscillation, the former at low frequency (around 60 GHz, with period ~ 16 ps) and the latter superimposed to the former at much higher frequency 1380 GHz (notice that the FFT frequency resolution ± 40 GHz is quite coarse due to the short time record to analyze). The low frequency oscillation can be ascribed to classical precessional dynamics, as it can be inferred by looking at the lower branch of the dispersion relation (6) (see also fig.1), which yields a frequency $|\omega_-| \to 57$ GHz (59 GHz using the classical exchange spin-wave dispersion relation $\omega = h_0 + l_{\rm ex}^2 k^2$).

On the other hand, one can see that the high frequency oscillation is associated with inertial nutation spin waves with the same wavelength 20 nm. This is also consistent with the upper branch of the dispersion relation ω_+ (see fig.1). As it can be seen in the upper panel of fig.6, these spin waves have much shorter lifetime which is apparently around 15 ps, after which they disappear due to damping. The spin wave lifetime (corresponding to exponential attenuation by more than two orders of magnitude) predicted by the developed theory (see eq.(14)) is $5/(\delta\omega\, \gamma M_s) \approx 19$ ps. This last simulation confirms the theoretical predictions and the results of the previously outlined numerical studies.

IV. CONCLUSIONS

In this work, we have investigated the possibility to excite ultra-short inertial spin with behavior that significantly deviates from that of the classical exchange spin-waves. A theoretical approach has been developed to determine the dispersion relation, the spatial decay and the lifetime of inertial spin waves as function of material and excitation parameters. It turns out that ultra-short (20 nm) inertial spin wave propagation in Cobalt films occurs at terahertz frequencies and admits a limiting speed in the order of 5500 m/s. Micromagnetic simulations both in frequency and time domains confirm the theoretical predictions concerning the possibility to excite finite speed propagation of such short waves in confined ferromagnetic nanodots by using terahertz ac fields with quite large amplitudes ($\sim$ 100 mT) such as those achievable with state-of-the art terahertz experimental setups. For these reasons, this study can be instrumental to stimulate and guide the design of experiments aiming to the observation of inertial spin wave dynamics.

ACKNOWLEDGMENTS

M.d'A., S.P., M.P., S.B. and C.S. acknowledge support from the Italian Ministry of University and Research, PRIN2020 funding program, grant number 2020PY8KTC.

[1] B. Dieny, I. L. Prejbeanu, K. Garello, P. Gambardella, P. Freitas, R. Lehndorff, W. Raberg, U. Ebels, S. O. Demokritov, J. Akerman, A. Deac, P. Pirro, C. Adelmann, A. Anane, A. V. Chumak, A. Hirohata, S. Mangin, S. O. Valenzuela, M. C. Onbaşlı, M. d'Aquino, G. Prenat, G. Finocchio, L. Lopez-Diaz, R. Chantrell, O. Chubykalo-Fesenko, and P. Bortolotti, Opportunities and challenges for spintronics in the microelectronics industry, Nature Electronics **3**, 446 (2020).

[2] E. Beaurepaire, J.-C. Merle, A. Daunois, and J.-Y. Bigot, Ultrafast spin dynamics in ferromagnetic nickel, Physical Review Letters **76**, 4250 (1996).

[3] B. Koopmans, M. van Kampen, J. T. Kohlhepp, and W. J. M. de Jonge, Ultrafast magneto-optics in nickel: Magnetism or optics?, Physical Review Letters **85**, 844 (2000).

[4] C. Stamm, T. Kachel, N. Pontius, R. Mitzner, T. Quast, K. Holldack, S. Khan, C. Lupulescu, E. F. Aziz, M. Wietstruk, H. A. Dürr, and W. Eberhardt, Femtosecond modification of electron localization and transfer of angular momentum in nickel, Nature Materials **6**, 740 (2007).

[5] C. D. Stanciu, F. Hansteen, A. V. Kimel, A. Kirilyuk, A. Tsukamoto, A. Itoh, and T. Rasing, All-optical magnetic recording with circularly polarized light, Physical Review Letters **99**, 047601 (2007).

[6] A. V. Kimel, B. A. Ivanov, R. V. Pisarev, P. A. Usachev, A. Kirilyuk, and T. Rasing, Inertia-driven spin switching in antiferromagnets, Nature Physics **5**, 727 (2009).

[7] A. Kirilyuk, A. V. Kimel, and T. Rasing, Ultrafast optical manipulation of magnetic order, Reviews of Modern Physics **82**, 2731 (2010).

[8] C.-H. Lambert, S. Mangin, B. S. D. C. S. Varaprasad, Y. K. Takahashi, M. Hehn, M. Cinchetti, G. Malinowski, K. Hono, Y. Fainman, M. Aeschlimann, and E. E. Fullerton, All-optical control of ferromagnetic thin films and nanostructures, Science **345**, 1337 (2014).

[9] C. Dornes, Y. Acremann, M. Savoini, M. Kubli, M. J. Neugebauer, E. Abreu, L. Huber, G. Lantz, C. A. F. Vaz, H. Lemke, E. M. Bothschafter, M. Porer, V. Esposito, L. Rettig, M. Buzzi, A. Alberca, Y. W. Windsor, P. Beaud, U. Staub, D. Zhu, S. Song, J. M. Glownia, and S. L. Johnson, The ultrafast Einstein–de Haas effect, Nature **565**, 209 (2019).

[10] M. Hudl, M. d'Aquino, M. Pancaldi, S.-H. Yang, M. G. Samant, S. S. Parkin, H. A. Dürr, C. Serpico, M. C. Hoffmann, and S. Bonetti, Nonlinear magnetization dynamics driven by strong terahertz fields, Physical Review Letters **123**, 197204 (2019).

[11] K. Neeraj, N. Awari, S. Kovalev, D. Polley, N. Z. Hagström, S. S. P. K. Arekapudi, A. Semisalova, K. Lenz, B. Green, J.-C. Deinert, I. Ilyakov, M. Chen, M. Bawatna, V. Scalera, M. d'Aquino, C. Serpico, O. Hellwig, J.-E. Wegrowe, M. Gensch, and S. Bonetti, Inertial spin dynamics in ferromagnets, Nature Physics **17**, 245 (2020).

[12] V. Unikandanunni, R. Medapalli, M. Asa, E. Albisetti, D. Petti, R. Bertacco, E. E. Fullerton, and S. Bonetti, Inertial spin dynamics in epitaxial cobalt films, Physical Review Letters **129**, 237201 (2022).

[13] M.-C. Ciornei, J. M. Rubí, and J.-E. Wegrowe, Magnetization dynamics in the inertial regime: Nutation predicted at short time scales, Physical Review B **83**, 020410(R) (2011).

[14] E. Olive, Y. Lansac, and J.-E. Wegrowe, Beyond ferromagnetic resonance: The inertial regime of the magnetization, Applied Physics Letters **100**, 192407 (2012).

[15] R. Mondal, M. Berritta, A. K. Nandy, and P. M. Oppeneer, Relativistic theory of magnetic inertia in ultrafast spin dynamics, Physical Review B **96**, 024425 (2017).

[16] C. Serpico, M. d'Aquino, G. Bertotti, and I. D. Mayergoyz, Quasiperiodic magnetization dynamics in uniformly magnetized particles and films, Journal of Applied Physics **95**, 7052 (2004).

[17] M. Bauer, J. Fassbender, B. Hillebrands, and R. L. Stamps, Switching behavior of a stoner particle beyond the relaxation time limit, Physical Review B **61**, 3410 (2000).

[18] G. Bertotti, I. Mayergoyz, C. Serpico, and M. d'Aquino, Geometrical analysis of precessional switching and relaxation in uniformly magnetized bodies, IEEE Transactions on Magnetics **39**, 2501 (2003).

[19] M. d'Aquino, W. Scholz, T. Schrefl, C. Serpico, and J. Fidler, Numerical and analytical study of fast precessional switching, Journal of Applied Physics **95**, 7055 (2004).

[20] T. Devolder, H. W. Schumacher, and C. Chappert, Precessional switching of thin nanomagnets with uniax-

ial anisotropy, in *Spin Dynamics in Confined Magnetic Structures III*, edited by B. Hillebrands and A. Thiaville (Springer Berlin Heidelberg, Berlin, Heidelberg, 2006) pp. 1–55.

[21] K. Neeraj, M. Pancaldi, V. Scalera, S. Perna, M. d'Aquino, C. Serpico, and S. Bonetti, Magnetization switching in the inertial regime, Physical Review B **105**, 054415 (2022).

[22] L. Winter, S. Großenbach, U. Nowak, and L. Rózsa, Nutational switching in ferromagnets and antiferromagnets, Physical Review B **106**, 214403 (2022).

[23] T. Kikuchi and G. Tatara, Spin dynamics with inertia in metallic ferromagnets, Physical Review B **92**, 184410 (2015).

[24] S. Giordano and P.-M. Déjardin, Derivation of magnetic inertial effects from the classical mechanics of a circular current loop, Physical Review B **102**, 214406 (2020).

[25] I. Makhfudz, E. Olive, and S. Nicolis, Nutation wave as a platform for ultrafast spin dynamics in ferromagnets, Applied Physics Letters **117**, 132403 (2020).

[26] A. M. Lomonosov, V. V. Temnov, and J.-E. Wegrowe, Anatomy of inertial magnons in ferromagnetic nanostructures, Physical Review B **104**, 054425 (2021).

[27] M. Cherkasskii, M. Farle, and A. Semisalova, Dispersion relation of nutation surface spin waves in ferromagnets, Phys. Rev. B **103**, 174435 (2021).

[28] R. Mondal and L. Rózsa, Inertial spin waves in ferromagnets and antiferromagnets, Physical Review B **106**, 134422 (2022).

[29] S. V. Titov, W. J. Dowling, Y. P. Kalmykov, and M. Cherkasskii, Nutation spin waves in ferromagnets, Physical Review B **105**, 214414 (2022).

[30] Z. Gareeva and K. Guslienko, Nutation excitations in the gyrotropic vortex dynamics in a circular magnetic nanodot, Nanomaterials **13**, 461 (2023).

[31] J.-E. Wegrowe and M.-C. Ciornei, Magnetization dynamics, gyromagnetic relation, and inertial effects, American Journal of Physics **80**, 607 (2012).

[32] M. d'Aquino and R. Hertel, Micromagnetic frequency-domain simulation methods for magnonic systems, Journal of Applied Physics **133**, 033902 (2023).

[33] M. d'Aquino, C. Serpico, G. Miano, and C. Forestiere, A novel formulation for the numerical computation of magnetization modes in complex micromagnetic systems, Journal of Computational Physics **228**, 6130 (2009), number: 17.

[34] M. d'Aquino, Magnetization Geometrical Integration Code, `http://wpage.unina.it/mdaquino/index_file/MaGICo.html`.

[35] G. Gubbiotti, M. Conti, G. Carlotti, P. Candeloro, E. D. Fabrizio, K. Y. Guslienko, A. Andre, C. Bayer, and A. N. Slavin, Magnetic field dependence of quantized and localized spin wave modes in thin rectangular magnetic dots, Journal of Physics: Condensed Matter **16**, 7709 (2004).

[36] M. d'Aquino, C. Serpico, and G. Miano, Geometrical integration of Landau–Lifshitz–Gilbert equation based on the mid-point rule, Journal of Computational Physics **209**, 730 (2005).